AN OPTIMIZATION ALGORITHM FOR EARTH FAULT LOCATION ON MV DISTRIBUTION FEEDERS

Trung Dung LE
CentraleSupélec-GeePs – France
trungdung.le@centralesupelec.fr

Marc PETIT
CentraleSupélec-GeePs – France
marc.petit@centralesupelec.fr

ABSTRACT

This paper presents an earth fault location algorithm based on optimization approach., which is developed for MV distribution networks with resistance-earthed neutral. The objective function is written based on relation between voltage and current measurements at substation, line parameters, fault distance and fault resistance. The optimization process is performed with MATLAB Optimization Toolbox that gives values to the last two variables. To deal with the heterogeneity of MV feeders, fault location is carried out successively on every homogeneous section lines and the optimal points of the different sections will be compared to give the final solution. The performance tests, which are performed on a MV CIGRE benchmark network, show encouraging results. In this study, impacts of load consumption uncertainty and of DG connection are also discussed.

INTRODUCTION

Fault location on MV distribution networks is an important application in outage management systems. However, this is a complex problem because of characteristics of the networks: unbalance, heterogeneity of feeder lines, numerous lateral branches and tapped loads. For years, algorithms for rapid and precise fault location [1] have been proposed in order to reduce the duration of power outages and improve the power quality, but it still remains a challenge to DSOs and researchers.

Among the proposed algorithms, impedance-based algorithms such as Takagi method, may prove to be more reliable and less expensive as their operation are based on phasor quantities of fundamental voltages and currents. The well-known Takagi method [2] is initially proposed for transmission networks to deal with the error introduced by fault resistance. The main idea is to use a polarizing current that is in phase with the fault current to eliminate the fault resistance term in the fault distance equation. In [3], the authors adapt this technique to locate earth faults on MV feeders. The estimation of fault current, based on zero-sequence network of MV grids and current measurements at the substation, is proposed as the polarizing quantity. Performances of the algorithm [3] are good, except for high values of fault resistance. In our previous work [4], an improvement in fault current estimation is proposed to better deal with high resistance faults. In the zero-sequence network, the MV line series impedance, which are often omitted in other algorithms, are taken into account in our work. The fault current and the fault distance are estimated thanks to an iterative process. The test results on a CIGRE benchmark network are promising.

In this paper, an alternative algorithm based on an optimization technique is proposed for earth fault location. By establishing the relation between measurements, line parameters, fault distance and fault resistance, the cost function will be built and solved with MATLAB Optimization Toolbox. The solution gives not only the fault distance but also the fault resistance. Details about the proposed algorithm is shown on the next section.

OPTIMIZATION FAULT LOCATION ALGORITHM

Homogeneous MV feeder

First of all, the main idea of the optimization fault location algorithm will be explained in case that the MV feeder is homogeneous. The single line to ground fault occurs on phase *a*. As shown in [4], based on PI models of section line between protection and fault, Kirchhoff's Voltage Law (KVL) equations can be written for the positive-, negative- and zero-sequence networks. By summing these equations, the following relation between voltage and current measurements at the substation, fault distance and fault resistance can be obtained:

$$V_S = x * z_1 * (I_S + K * I_{0S}) - j * 0.5 * \omega * x^2 * z_1 * c_1 * (V_S + K_C * V_{0S}) + R_F * I_F \quad (1)$$

Where

V_S, I_S are the faulty phase voltage and current respectively measured by the protection at the substation (S).

V_{0S}, I_{0S} are the zero-sequence voltage and current respectively measured by the protection at the substation (S).

x is the distance (km) from the substation to fault

I_F is the fault current (phase *a*) at the fault point

R_F is the fault resistance

$K = (z_0 - z_1)/z_1$ and $K_C = (z_0c_0 - z_1c_1)/(z_1c_1)$

z_1, z_2, z_0 are the per unit length impedances (Ω/km) in the positive-, negative- and zero-sequence networks

c_1, c_2, c_0 are the per unit length capacitances (F/km) in the positive-, negative- and zero-sequence networks

$\omega = 2\pi f$ with $f = 50$ Hz

From (1), the objective function can be written as:

$$f(x,R_F) = |x * z_1 * (I_S + K * I_{0S}) - j * 0.5 * \omega * x^2 * z_1 * c_1 * (V_S + K_C * V_{0S}) + R_F * I_F - V_S| \quad (2)$$

The multivariable optimization problem is:

$$\min f(x,R_F) \quad (3)$$

Subject to

$$\begin{cases} 0 \le x \le L \\ R_F \ge 0 \end{cases}$$

L is the length of the faulty feeder. The problem can be solved with Optimization Toolbox of Matlab. The fault distance x and fault resistance R_F will be given at the optimal point.

In (2), the fault current I_F can be estimated based on the zero-sequence network of the MV grid (Fig. 1) and it will be shown that I_F is also a function of the fault distance x.

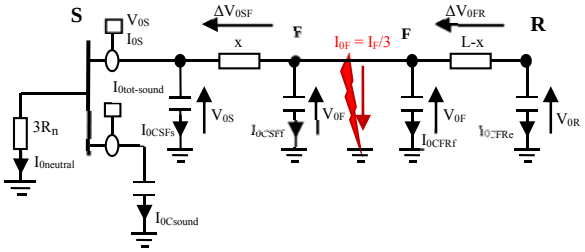

Figure 1. Generic zero-sequence network of MV distribution grids

As can be seen in Fig. 2, the faulty feeder can be divided in two section lines: one from the substation (S) to the fault (F) and the other from the fault point (*F*) to the remote end (R). The other feeders are represented by an aggregated capacitor. The MV distribution grid has its grounding system at the substation with resistive grounding (R_n). The fault current will be determined as follows:

$$I_F = -3 * \left(I_{0neutral} + I_{0Csound} + \sum I_{0Cfaulty} \right) \quad (4)$$

where $I_{0neutral}$ is the zero-sequence neutral current

$I_{0Csound}$ is the sum of zero-sequence currents of all sound feeders

$\sum I_{0Cfaulty}$ is the total zero capacitive current of the *two* section SF and FR of the faulty feeder

$I_{0neutral}$ and $I_{0Csound}$ are measured by current sensors at the substation. $\sum I_{0Cfaulty}$ will be calculated from the zero-sequence voltages V_{0S}, V_{0F}, V_{0R} respectively at nodes S, F and R. It should bear in mind that for the proposed algorithm, the series impedances are taken into account and $V_{0S} \neq V_{0F} \neq V_{0R}$. In fact, V_{0S} is measured at the substation. Voltage information of other nodes will be determined from V_{0S} and the voltage drop between substation and the node in question. The voltage drops depend on fault distance x. As a result, the calculated voltages V_{0F} and V_{0R} depends also on fault distance. Finally, $\sum I_{0Cfaulty}$ and I_F are consequently a function of x.

Heterogeneous MV feeder with lateral sections

Real MV feeders are seldom homogeneous, but rather consist of heterogeneous sections, with tapped loads and lateral lines. To cope with this complexity, the fault location procedure proposed in the previous work [4] will be reused here. In brief, the algorithm will be executed for all possible paths of the faulty feeder, each goes from substation to one remote end of the feeder. It should be reminded that a MV feeder may have many remote ends from which there is no more downstream node. All lateral section lines with respect to a path will be reduced to an equivalent impedance connected to the bifurcation. For this calculation, constant impedance load model will be used. On each path that consists of homogeneous section lines, the fault location procedure will be run in each homogeneous section successively from substation to the remote end. The required voltage and current information at the beginning of each new section will be calculated from the information of the adjacent upstream section. The fault current should also be recalculated when the fault location algorithm is run on the new downstream section. The optimal points of all sections will be compared to each other to find the final solution of the path. The algorithm gives in this manner one solution for each path. There may be many paths and as a result, the algorithm may give more than one solution. This procedure is summarized in the flowchart of the Fig. 2.

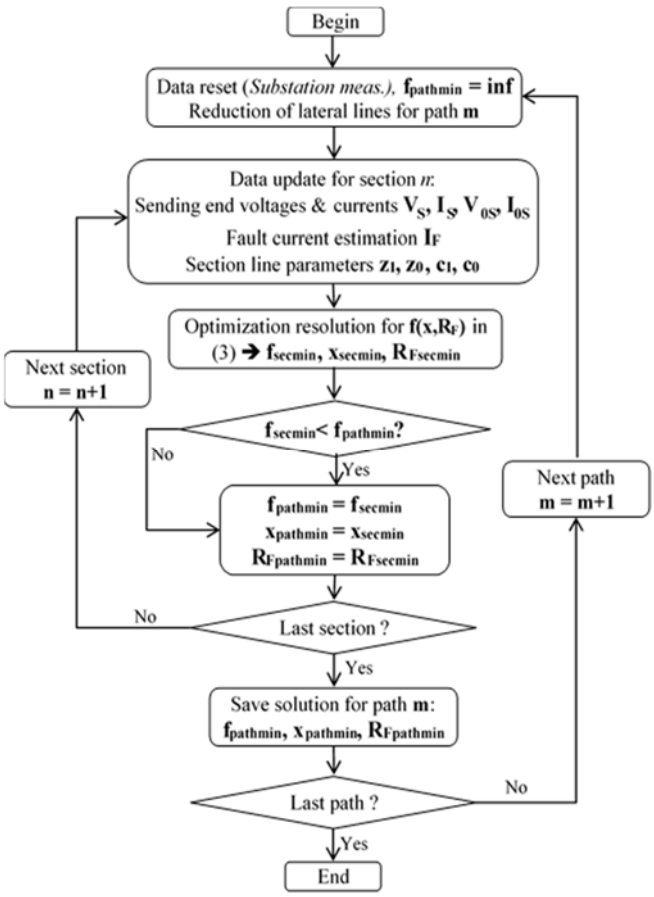

Figure 2. Fault location algorithm on heterogeneous feeders

TEST NETWORK AND RESULTS

CIGRE benchmark MV networks

The proposed algorithm is tested with fault data generated from simulations on a CIGRE benchmark MV network [5]. The simulations are carried out in the SimPowerSystems Toolbox of Matlab/Simulink. The network single line diagram is shown in Fig. 3.

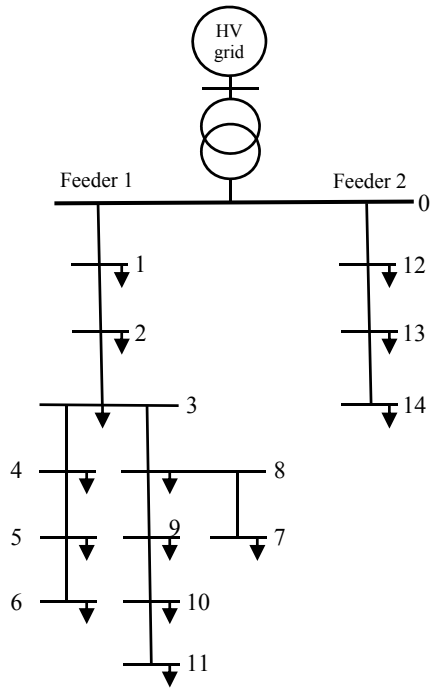

Figure 3. CIGRE benchmark MV network

There are two "mixed" radial feeders, each consists of overhead lines and underground cables. Details of grid parameters are given in Appendix. Some key parameters are the following:

- Feeder 1: composed of 2.82 km of overhead lines and 11.84 km of underground cables, 5.7 MVA of total loads; 11 homogeneous section lines with bifurcation. 3 possible paths for fault location algorithm: node 0-1-2-3-4-5-6 (path 1), node 0-1-2-3-8-7 (path 2), node 0-1-2-3-8-9-10-11 (path 3).
- Feeder 2: composed of 7.88 km of overhead lines and 0.32 km of underground cables, 1.2 MVA of total loads; 3 homogeneous section lines and single possible path: node 0-12-13-14 (path 4)

Fault position is varied in simulations: the fault is put on one of the 14 section lines of the two feeders in each simulation, from the first section to the last successively. On each section, the fault is simulated at three positions: at 10%, 50% and 90% of the section length. For each position, the fault resistance R_F will also be varied from 0 to 1000 Ω (7 values of R_F: 0, 10, 50, 100, 200, 500, 1000 Ω). As a result, there will be in total 294 simulations that will be carried out. As mentioned previously, substation voltages and currents at the head of the two feeders and on the neutral grounding are "measured".

Test results

In this study, all network data (line impedances, load consumptions) are supposed to be available for fault location and equal to ones given in Appendix. Voltage and current measurements are supposed to be perfect. To give an idea about the solution that may be given by the proposed algorithm, an example of results is depicted in the Table I with the fault that is simulated at 10% of the length of Section 9-10 and R_F = 200 Ω. Thus the fault is at 9257 m from the substation.

TABLE I. FAULT LOCATION RESULTS FOR FAULT ON SECTION 9-10 (R_F = 200 Ω), FAULT DISTANCE = 9257 METERS

Found section	Found distance (m)	Estimated fault resistance (Ω)	Status	Distance error (m)
5-6 (path 1)	9229	200.1	Wrong	NA
8-7 (path 2)	9193	200.5	Wrong	NA
9-10 (path 3)	9188	200.3	OK	70

The algorithm is run on all three paths of the feeder 1 and gives a solution for each path. As can be seen in Table I, a solution consists of found section line on the path, the fault distance from the substation and the fault resistance. To evaluate the algorithm performances, the status "OK" will be indicated next to the solution if the found section is the real faulty one. The distance error will also be calculated as the difference between the found distance and the real fault distance from the substation. Otherwise, the status "Wrong" will be indicated. The results will be considered as good if for a given simulated fault, there is at least one solution with status "OK". In the table I, the third solution on path 3 is the section 9-10, which is the real faulty section with 70m of error. The status is OK so the results for this fault are good.

Analysis on all 294 simulations shows good performances of the proposed optimization algorithm: in 93.2% of test cases, it gives the good results or in other words, the faulty section is correctly identified. This rate (93.2%) is slightly higher than one given the Modified Takagi method (91.5%) described in our previous work [4]. To show the impact of fault resistance R_F on algorithms' performances, the accuracy rates in faulty section identification as function of R_F depicted in Table II. As it can be seen, the two algorithms can correctly identify the faulty section for all faults with $R_F \leq 100\Omega$. For faults with higher resistance, performances are

degraded. Further study shows that the two algorithms are in fact able to detect the real faulty section or at least the adjacent sections with respect to the real one for all test cases.

TABLE II. ACCURACY IN FAULTY SECTION IDENTIFICATION (%)

R_F (Ω)	0	10	50	100	200	500	1000
Optimization algorithm	100	100	100	100	95.2	83.3	73.8
Modified Takagi algorithm	100	100	100	100	92.9	78.6	69.0

Fig. 4 shows the box plot for errors in fault distance estimation in function of fault resistance for the proposed optimization algorithm. The bottom and the top of each box indicate the first and third quartiles. The red band inside each box shows the median of errors. The ends of the whiskers represent the 5th and 95th percentile of errors. For faults with $R_F \leq 200\Omega$, the algorithm gives a pretty precise fault distance: the median of error is smaller than 50m with regard to the real fault position. The distance error increases for the higher values of R_F but the median remains under 160m for all test cases. Another remark after analyzing all the test cases is that the distance error depends on fault distance: the algorithm will produce more errors for faults at the remote end sections than ones at the head of the feeders.

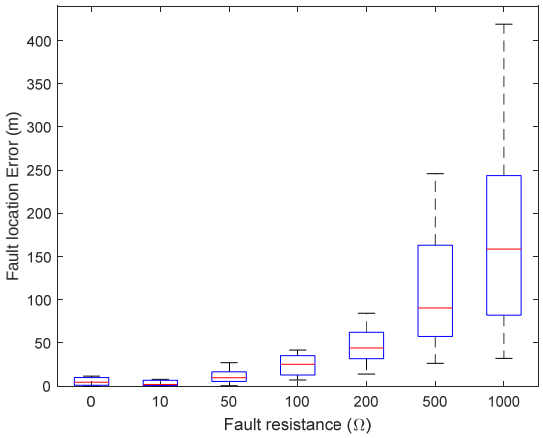

Figure 4. Errors in fault distance estimation in function of fault resistance – Optimization Algorithm

.

Impact of uncertainty in load consumptions

Load consumptions are permanently varied and the real-time data are not generally available. To study the robustness of the optimization algorithm with regards to the load uncertainty, the fault location algorithm will be run again for all 294 simulated fault positions but with imperfect load data: uncertainty will be introduced to the load consumptions (i.e. to the active and reactive powers of each node shown in the data table in Appendix) and there will be 200 draws for each fault position. The uncertainty will follow the Gaussian distribution with standard deviation of 16.7% of the mean values of power consumptions shown in Appendix. Results show that the proposed algorithm can only identify the real faulty section line in 90.8% of cases. If the adjacent sections to the real faulty section are taken into account as the good results, the accuracy rate will increase to 99.6%. The box plot of distance errors is shown in Fig. 5. As it can be seen, the load uncertainty increases greatly the upper whiskers (95th percentile) as compared to ones on Fig.4. However, the tops of the boxes (3rd quartile) increases only slightly and the medians stay nearly at the same level. It can be said that the algorithm is rather robust with regards to uncertainty in load data.

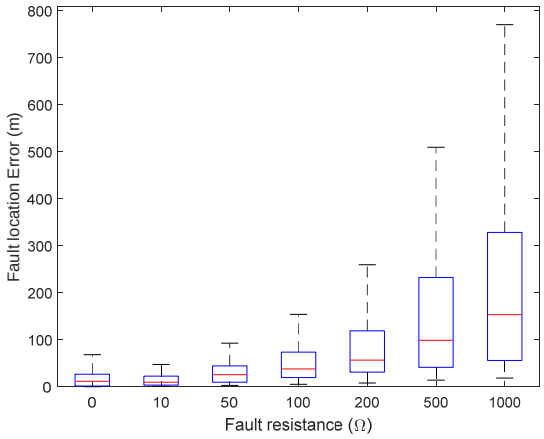

Figure 5. Impact of Load uncertainty on errors in fault distance estimation – Optimization Algorithm

Impact of DGs

In France, DGs are connected to MV grids through a star/delta coupling transformer with delta connection on the MV side. Hence there is no MV grounding point created by DGs and the generators don't contribute to zero-sequence currents. However, DG fault response is different compared to normal loads and they may still have impacts on positive- and negative-sequence currents. Consequently, the presence of DGs may alter the fault location results. To better understand DG impacts, a 5 MVA synchronous generator is added to the CIGRE test network. DG parameters are given in Appendix. The connection point is first chosen at node 2 (near to the substation). Simulations on Simulink/SimPowerSystems are run again on the MV grid with DG. The optimization fault location algorithm is also run again with the new recorded voltage and current data from the simulations. In a first approach, DG is modelled – in the fault location data – as a negative load (i.e. load that consumes negative powers). The analyses show that the accuracy rate in faulty section identification decreases from 93.2% without DG to 80.6% with DG at node 2. The accuracy rate in presence

of DG will be 98.3% if the adjacent sections to the faulty section are also taken into account. On the other hand, the median of distance errors increase to 128m (from 20m without DG).

In case that the DG is connected at node 9 (near the remote end – node 11), the same process is carried out. The accuracy rate of faulty section identification is 81.3% without adjacent sections and 94.9% with adjacent sections to the real faulty section taken into account. respectively. The median of distance errors is 71m. A more detailed comparison of distance errors is shown in Fig. 6 for all three cases: no DG, DG at node 2 and DG at node 9.

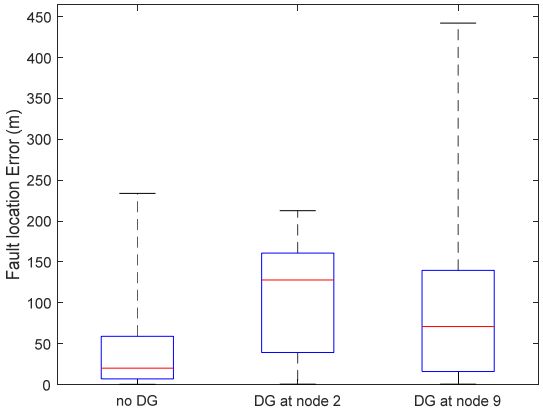

Figure 6. Impact of DG on errors in fault distance estimation – Optimization Algorithm

CONCLUSIONS

In this paper, an optimization algorithm for fault location on distribution networks is proposed. The algorithm requires only voltages and currents measured at the substation and gives good performances. In 93.2% of test cases, the proposed algorithm is able to correctly identify the real faulty section. It should be noted that in the fault location process, the network and load data are supposed to be perfectly known. Further study on impact of load consumption uncertainty shows that the algorithm is also robust to the uncertainty: the faulty section line is correctly detected in 90.8% of test cases. The DG impacts are greater: the faulty section is correctly identified in only 80.6% and 81.3% of cases for 5 MVA DG connected at node 2 of cases at node 2 and at node 9 respectively. This may be due to the DG model (negative load) that has been simplified in the algorithm. This point should be further analysed in the future works.

REFERENCES

[1] M.M. Saha, J.J. Izykowski, E. Rosolowski, 2010, *Fault Location on Power Networks*, Springer.

[2] T. Takagi, Y. Yamakoshi, M. Yamaura, R. Kondow, and T. Matsushima, 1982, "Development of a New Type Fault Locator Using the One-Terminal Voltage and Current Data", *IEEE Trans. on Power Apparatus and Systems,* Vol. PAS-101, No. 8.

[3] R. Marguet, 2015, "Improved Fault Localization Method for Electrical Power Distribution Networks", *PhD Dissertation*, Univ. de Grenoble.

[4] T.D. Le, M. Petit, 2016, "Earth Fault Location based on a Modified Takagi Method for MV Distribution Networks", *Proceedings of IEEE ENERGYCON*, Leuven (Belgium).

[5] P. Janssen, 2014, "Monitoring, protection and fault location in power distribution networks using system-wide measurements", *PhD Dissertation*, Univ. Libre de Bruxelles.

APPENDIX

Test network characteristics:

- HV network: 63 kV, P_{cc} = 600 MVA, X/R = 10
- HV/MV Transformer: 63/20 kV, S_{rated} = 36 MVA, u_{cc}=17%
- Neutral impedance: R_n=40 Ω (resistive grounding).
- DG (synchronous generator) parameters: round rotor, S_n=5MVA, r_s=0.005, x_d=x_q=2.0, x_d'=x_q'=0.25, x_d"=x_q"=0.2, x_l=0.05, T_d'= 0.5s, T_q'= 0.1s, T_d"=0.03s, T_q"=0.048s
- DG Coupling transformer: 400V/20kV, S_n = 5MVA, u_{cc}=6%
- Line characteristics & load data:

Fbus	Tbus	Length (km)	r_1 (Ω/km)	x_1 (Ω/km)	r_0 (Ω/km)	x_0 (Ω/km)	c_1 & c_0 (μF/km)	Load (MVA) at Tbus
0	1	0.32	0.34	0.13	1.02	0.52	0.32	0.54
1	2	2.82	0.58	0.37	0.77	1.1	0.02	0.54
2	3	4.42	0.16	0.11	0.49	0.45	0.32	0.54
3	4	0.61	0.26	0.12	0.79	0.48	0.32	0.45
4	5	0.56	0.35	0.13	1.06	0.52	0.32	0.75
5	6	1.54	0.34	0.13	1.01	0.5	0.32	0.57
3	8	1.3	0.17	0.12	0.52	0.46	0.32	0.61
8	9	0.32	0.34	0.13	1.02	0.52	0.32	0.68
9	10	0.77	0.4	0.13	1.2	0.53	0.32	0.57
10	11	0.33	0.37	0.13	1.1	0.53	0.32	0.34
8	7	1.67	0.29	0.12	0.88	0.49	0.32	0.09
0	12	0.32	0.34	0.13	1.02	0.52	0.32	0.54
12	13	4.89	0.34	0.36	0.45	1.07	0.02	0.04
13	14	2.99	0.2	0.12	0.27	0.37	0.02	0.60